Soft Template Synthesis of Highly Crystalline Microscale Nanotubules of PbO

Qin Zhou, Xiaoying Liu, Ling Liu, Yanguang Li, Zhiyu Jiang,* and Dongyuan Zhao
Department of Chemistry, Shanghai Key Laboratory of Molecular Catalysis and Innovative Materials,
Fudan University, Shanghai 200433, P. R. China

(Received May 16, 2005; CL-050648)

Highly crystalline microscale nanotubules of PbO with diameters in the range of 90–600 nm and lengths up to 15 µm have been synthesized by using triblock copolymer P123 as the template via a practical electrodeposition process.

One-dimentional (1D) structures such as nanotubes and nanowires have been a subject of intensive research because of their novel properties and intriguing applications in electronic, magnetic, optical, and micromechanical devices.[1,2] There are many reports about the synthesis of 1D metals and metal oxides, for example, nanowires of Pd,[3] Ag,[4] BiSb,[5] and ZnO,[6] nanobelts of ZnO, SnO_2, and In_2O_3,[7] and nanotubes of Pt, Ag, Pd,[8] Pd/Ag,[9] TiO_2,[10] ZrO_2,[11] WO_3, MnO_2, Co_3O_4, and V_2O_5.[12] While most of these studies deal with noble or transition metals, relatively less is known about the 1D nanostructures of main group elements with only a few studies including nanobelts of PbO_2,[13] nanoribbons of SnO_2,[14] and nanowires of GeO_2,[15] In_2O_3,[16] MgO,[17] and Ga_2O_3.[18] Previous researchers have shown that 1D nanostructures are more prone to charge transport than the bulk crystalline structures.[19] Although there are many reports about nanotubules, to the best of our knowledge, studies about the preparation of lead oxides with 1D nanostructures hence their subsequent applications in nanoscale electronic devices have been relatively few. In this case, synthesis of 1D PbO nanostructures is very important. Recently, a very large variety of oxides have been prepared by electrodeposition. This technique presents some interesting advantages when compared with other methods such as chemical vapor deposition, sputtering, etc. The deposition occurs at low temperature and at atmospheric pressure; the experiments are simple to perform and the instruments are inexpensive and readily available; the film thickness can be directly monitored by the charge consumed during the deposition process.[20,21]

In a galvanostatic synthesis, a delicate control can be exercised over the rate of the reaction leading to deposition with good adhesion and a controlled morphology.[21] We have demonstrated herein that tubules of lead oxide PbO could be prepared through galvanostatic electrodeposition of Pb followed by a spontaneous oxidation in air. In this study, an amphiphilic triblock copolymer $HO(CH_2CH_2O)_{20}(CH_2CH(CH_3)O)_{70}(CH_2CH_2O)_{20}H$ (designated as $EO_{20}PO_{70}EO_{20}$; Pluronic P123, BASF) was employed as a soft template. Different reaction conditions (e.g., the concentration of P123, HNO_3) were also found to have a profound impact on the morphologies of the finial products. In particular, it was found that controlling the amount of HNO_3 provided a good way to adjust the morphology of the resultant nanostructures.

A typical electroplating solution was prepared as following: 21 g of 0.1 M $Pb(NO_3)_2$, was mixed with 8 g of ethanol, 0.6 g of P123, and 1.1 g of HNO_3. The mixture was stirred to form a clear solution after 5 min. An electrolysis copper and a cast lead plate were used as the cathode and anode, respectively. The electrodeposition was conducted using a galvanostatic electroplating circuit. Constant current across the two spaced electrodes (2 cm) was applied for 60 min with a current density of 3–13 mA·cm^{-2} at 40 °C. After deposition, the electrode was washed with ethanol for 5 times in order to remove the surfactant. The electrode was subsequently dried in dry air.

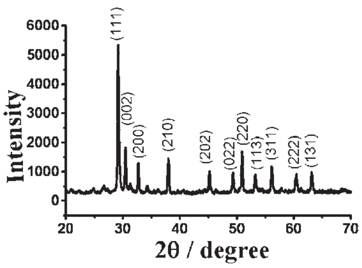

Figure 1. XRD pattern of the typical sample.

The X-ray diffraction (XRD) pattern of an obtained typical material is shown in Figure 1. Well-resolved diffraction peaks can be observed, indicating good crystallinity of the resultant materials. Its peak positions agree well with those of PbO in the orthorhombic phase (JCPDS No. 05-570). The lattice constants are $a = 5.48$ Å, $b = 4.75$ Å, $c = 5.89$ Å, respectively. The XRD patterns indicates that metallic lead exposed to air is easily oxidized, which has also been demonstrated by previous researchers that metallic Pb was primarily deposited, ruling out the effect of O_2 and NO_3^- reduction and was then rapidly

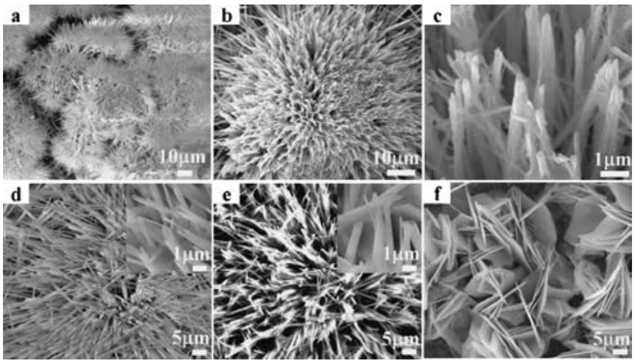

Figure 2. SEM images of lead oxide electrodeposited from different solutions containing (a–c) 21 g of 0.1 M $Pb(NO_3)_2$, 8 g of ethanol, 0.6 g of P123, and 1.1 g of HNO_3, with b and c the higher magnification images of a; (d) 21 g of 0.1 M $Pb(NO_3)_2$, 8 g of ethanol, 0.6 g of P123, and 0.7 g of HNO_3; (e) 21 g of 0.1 M $Pb(NO_3)_2$, 8 g of ethanol, 2.9 g of P123, and 1.1 g of HNO_3; (f) 21 g of 0.1 M $Pb(NO_3)_2$, 8 g of ethanol, 2.0 g of P123, and no HNO_3.

oxidized and converted into β-PbO upon exposure to air as a result of reaction at the solid/gas interface after the electrodeposition.[22]

Figure 2a shows the representative low-magnification scanning electron microscope (SEM) image of the PbO product, in which aggregated bundles can be observed. It is very possible that nucleation of a solid phase initially occurred on some spots of the substrate surface and subsequent crystal growth proceeded radically in different directions at the bulk solution. This radial structure can be more clearly seen in Figure 2b, displaying an individual flower-like aggregation. Figure 2c shows the SEM image of the product at higher magnification. It can be seen that the diameter of PbO tubules is in the range of 90–250 nm, and the length of tubules can reach 15 µm. For comparison, samples obtained from other synthetic solutions with different concentrations of HNO_3 and P123 are also shown. When the amount of HNO_3 was decreased to 0.7 g, or the amount of P123 was increased to 2.9 g, high-magnification SEM images (inset in Figures 2d and 2e) show similar tubules structure with the diameters in the range of 90–600 nm and with degraded uniformity. EDX analysis of sample (Figure 2e) shows that there is much more carbon in the PbO tubules (5 wt %) compared with that in the sample shown in Figures 2a–2c (undetectable), implying that P123 molecules may tend to adsorb on the surface of tubules under this synthetic condition. It is thus postulated that the film growth is relatively retarded as compared to that shown in Figure 2b, because of the higher ratio of P123 to HNO_3. In this case, the P123 molecules could be deposited together with sample and intermingle in the sample crystal structure. From a solution without HNO_3 at all, PbO product was observed as sheets interwoven to each other (Figure 2f).

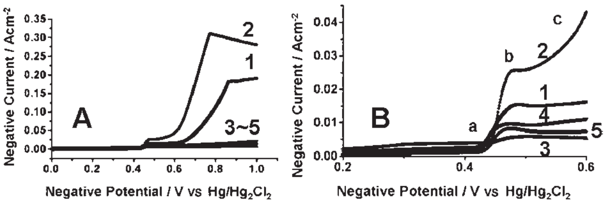

Figure 3. The lead polarization curves from different solutions. B is the local magnification of A. (1) 0.1 M $Pb(NO_3)_2$; (2) 21 g of 0.1 M $Pb(NO_3)_2$ and 1.1 g of HNO_3; (3) 21 g of 0.1 M $Pb(NO_3)_2$, 8 g of ethanol, and 0.6 g of P123; (4) 21 g of 0.1 M $Pb(NO_3)_2$, 8 g of ethanol, 0.6 g of P123, and 1.1 g of HNO_3; (5) 21 g of 0.1 M $Pb(NO_3)_2$, 8 g of ethanol, 0.6 g of P123, and 0.7 g of HNO_3. Scan rate: $v = 5\,\mathrm{mV{\cdot}s^{-1}}$, Temperature: 40 °C.

It can be seen that the concentrations of HNO_3 and P123 are two key factors to achieve the tubular morphology. In order to investigate their roles in the deposition process, the polarization measurement of Pb electrodeposited from 0.1 M $Pb(NO_3)_2$ electrolyte with and without HNO_3 and P123 has been carried out. Figure 3 shows the curves of current density versus potential for different electrolytes. The curves can be divided into three parts, the first part is before point a, the second part is ab section, and the third part bc section. The hydrogen starts to form at point a and is generated quickly in ab section. After point b, Pb particles begin to deposit and as the major product in bc section. It can be clearly seen that the addition of HNO_3 favors while P123 inhibits the generation of hydrogen, which can be attributed to the nonionic surfactant nature of P123 that can adsorb on the surface of the cathodic Cu, thus prevent the hydrogen generation. The addition of HNO_3 has no contribution to the formation of PbO and only supplies hydrogen ions. So the competition of hydrogen evolution with the electrodeposition of Pb is important during the synthesis. It is worth noting that block copolymer P123 could have another role in the synthesis: as a nonionic surfactant, it could adsorb on the surface of Cu and block some space and/or on the surface of Pb materials during the reaction, hence modulate the growth kinetics of the Pb seeds, which is controlled probably by its different adsorption energies on various crystallographic facets of Cu and/or Pb. Similar phenomena have been observed in the growth of silver nanostructure by using PVP as a soft template.[4] During the growth period, the crystallization rate is so high that a preferential growth dominates. The inorganic and organic nutrients are consumed rapidly near the nuclei, leading to the growth of radial structures.

In summary, we report here a practical approach to synthesize PbO microscale nanotubules via electrodeposition by using nonionic surfactant P123 as a template. It is the first time that PbO tubules with orthorhombic structure can be achieved by electrodeposition. By controlling the relative amount of P123 and HNO_3, the morphology of the resultant nanostructures can be adjusted.

We acknowledge financial support of this work by the Natural Science Foundation of China (NSFC).

References

1 F. Krumeich, H. J. Mubr, M. Niederberger, F. Bieri, B. Schnyder, and R. Nesper, *J. Am. Chem. Soc.*, **121**, 8324 (1999).
2 W. Tremel, *Angew. Chem., Int. Ed.*, **38**, 2175 (1999).
3 D. Wang, W. Zhou, B. F. McCaughy, J. Eric Hampsey, X. Ji, Y. Jiang, H. Xu, C. J. Brinker, and Y. Lu, *Adv. Mater.*, **15**, 130 (2003).
4 Y. Sun and Y. Xia, *Science*, **298**, 2176 (2002).
5 A. L. Prieto, M. M. Gonzalez, J. Keyzni, R. Gronsky, T. Sands, and A. M. Stacy, *J. Am. Chem. Soc.*, **125**, 2388 (2003).
6 M. H. Huang, Y. Wu, H. Feick, N. Tran, E. Weber, and P. Yang, *Adv. Mater.*, **13**, 113 (2001).
7 Z. W. Pan, Z. R. Dai, and Z. L. Wang, *Science*, **291**, 1947 (2001).
8 T. Kijima, T. Yoshimura, M. Uota, T. Ikeda, D. Fujikawa, S. Mouri, and S. Uoyama, *Angew. Chem., Int. Ed.*, **43**, 228 (2004).
9 Y. Sun, B. Wiley, Z. Li, and Y. Xia, *J. Am. Chem. Soc.*, **126**, 9399 (2004).
10 P. Hoyer, *Langmuir*, **12**, 1411 (1996).
11 C. N. R. Rao, B. C. Satishkumar, and A. Govindaraj, *Chem. Commun.*, **1997**, 158.
12 B. BLakashmi, P. K. Dorhout, and C. R. Martin, *Chem. Mater.*, **9**, 857 (1997).
13 Z. W. Pan, Z. R. Dai, and Z. L. Wang, *Appl. Phys. Lett.*, **80**, 309 (2002).
14 J. Q. Hu, X. L. Ma, N. G. Shang, Z. Y. Xie, N. B. Wong, C. S. Lee, and S. T. Lee, *J. Phys. Chem. B*, **106**, 3823 (2002).
15 Z. G. Bai, D. P. Yu, H. Z. Zhang, Y. Ding, X. Z. Gai, Q. L. Hang, G. C. Xiong, and S. Q. Feng, *Chem. Phys. Lett.*, **303**, 311 (1999).
16 P. Yang and C. M. Lieber, *J. Mater. Res.*, **12**, 2981 (1997).
17 Y. C. Choi, W. S. Kim, Y. S. Park, S. M. Lee, D. J. Bae, Y. H. Lee, G. S. Park, W. B. Choi, N. S. Lee, and J. M. Kim, *Adv. Mater.*, **12**, 746 (2000).
18 B. Tian, X. Liu, H. Yang, S. Xie, C. Yu, B. Tu, and D. Zhao, *Adv. Mater.*, **15**, 1370 (2003).
19 W. U. Huynh, J. J. Dittmer, and A. P. Alivisatos, *Science*, **295**, 2425 (2002).
20 Th. Pauporté, A. Goux, A. Kahn-Harari, N. de Tacconi, C. R. Chenthamarakshan, K. Rajeshwar, and D. Lincot, *J. Phys. Chem. Solids*, **64**, 1737 (2003).
21 G. H. A. Therese and P. V. Kamath, *Chem. Mater.*, **12**, 1195 (2000).
22 S. Sawatani, S. Ogawa, T. Yoshida, and H. Minoura, *Adv. Funct. Mater.*, **15**, 297 (2005).